Green Chemistry

Accepted Manuscript

This article can be cited before page numbers have been issued, to do this please use: B. Dutta, S. March, L. Achola, S. Sahoo, J. He, A. Shirazi Amin, Y. Wu, S. POGES, P. Alpay and S. L. Suib, *Green Chem.*, 2018, DOI: 10.1039/C8GC00862K.

ROYAL SOCIETY OF CHEMISTRY

rsc.li/green-chem

View Article Online
DOI: 10.1039/C8GC00862K

Journal Name

COMMUNICATION

Mesoporous Cobalt/ Manganese Oxide: A Highly Selective Bifunctional Catalyst for Amine–Imine Transformations

Received 14th March 2018

Biswanath Dutta,[a] Seth March,[a] Laura Achola,[a] Sanjubala Sahoo,[b] Junkai He,[b] Alireza Shirazi Amin,[a] Yang Wu,[b] Shannon Poges,[a] S. Pamir Alpay,[b] and Steven L. Suib[a, b, *]

www.rsc.org/

Herein, we discuss a heterogeneous catalytic protocol using cobalt doped mesoporous manganese oxide for amine-alcohol cross-coupling to selectively produce symmetric or asymmetric imines. Thorough investigations on the surface chemistry and physical properties of the material revealed its outstanding oxidation-reduction properties and reaction mechanism which was supported by quantum mechanical calculations done by using density functional theory (DFT).

Imines, also known as Schiff bases, are an essential class of compounds for their versatile applications in the production of heterocyclic chemicals, pharmaceutically and biologically active compounds, and fine chemicals.[1–3] The C=N bond in imines, being chemically unstable, are widely used for various organic transformations such as reduction, addition, and cyclization.[1,4] Conventionally, imines are produced from the condensation reaction of amines to activated aldehydes in the presence of various dehydrating agents, bases and Lewis acid catalysts which limit their industrial applications.[5] Over the past decade, extensive research has been devoted to facilitating the acceptor-less process of synthesizing imines. During this development various alternative approaches have been marked to synthesize different imines, such as i) the self-coupling of amines, ii) oxidation of secondary amines and iii) coupling of alcohols to amines.[6] Though the latter two are used for synthesizing asymmetric imines, the oxidation of secondary amines is not a useful way due to the requirement of their prior access.[1] Consequently, the alcohol-amine coupling is considered to be the only effective tool for selectively synthesizing asymmetric imines.

Several approaches have been employed for this transformation using stoichiometric oxidants such as various iridium-complexes,[7] and periodates.[8] The generation of toxic waste and its complicated separation method make these processes industrially impractical.[9] Hence, aerobic oxidation methods that use air as the sole oxidant are considered to be most economical and environmentally benign.[10–12] Direct use of air being difficult, a mediator or co-catalyst is highly important. Numerous catalytic systems have been reported to date to perform that coupling reaction efficiently. Popular protocols can be categorized as, 1) precious metal-based systems, such as Au,[13] Ag,[14] Pd,[15] Pt,[16] and Ru;[17] 2) non-precious metal-based systems, such as Mn,[12,18] Fe,[19] Cu,[20] and CeO_2;[21] and 3) photocatalysts such as TiO_2,[22] and $BiVO_4$/g-C_3N_4.[23] Despite obtaining good conversions from some systems, most of them suffered from the use of i) precious metals,[13–17] ii) toxic catalysts,[8,20] iii) complicated synthetic procedure,[24] iv) prolonged reaction time,[12] v) harsh reaction conditions, such as high pressure,[25] or temperature,[16] vi) high energy light irradiation,[23] and vii) oxidative promoters.[20] Hence, the development of a catalytic system is highly important which can minimize all above-mentioned issues and evolve as a cost-effective, atom economic, additive free, and highly reusable procedure, following the foundations of green chemistry.[26]

In the past two decades, the use of heterogeneous catalytic procedures has rapidly evolved due to their i) excellent reusability, ii) high cost-economy, and ii) minimum waste generation.[27] Therefore, we aimed to develop a highly efficient, heterogeneous catalytic system for amine-alcohol cross-coupling reactions.

In recent years, mesoporous manganese oxide (meso-MnOx) based systems have been extensively studied for their superior heterogeneous catalytic activity for various organic transformations, such as a) alcohol oxidation,[28] b) homo-coupling of amines to imines,[29] c) anilines to aromatic azo compounds,[30] d) sp^2-C to sp^2-C coupling,[31] and e) alkane oxidations.[32] The superior catalytic activity of meso-MnOx over the other systems, such as meso-CoOx, meso-FeOx, and meso-NiOx, was recognized due to: i) weakest metal-oxygen bond,[33] ii) the excellent redox properties due to the prevalence of multi-valency, iii) abundant active sites (Mn^{3+}), iv) enhanced lattice oxygen content, and v) high mobility of lattice oxygens.[31] Despite such development of manganese oxide catalysis, relatively higher reaction time was recorded for amine to alcohol coupling.[12,18] Controlling the selectivity for benzylic alcohol-amine coupling was also found to be challenging.[18,29] These studies resulted in an increasing demand for enhancing catalytic reactivity and selectivity of hetero coupled products. We have made an effort to solve these issues by increasing the surface defects of the catalyst. This is the first example of a heterogeneous system which

[a] Department of Chemistry, University of Connecticut, Storrs, CT 06269 (USA).

[b] Institute of Material Science, University of Connecticut, Storrs, CT 06269 (USA).

View Article Online
DOI: 10.1039/C8GC00862K

exclusively produces cross-coupled products from benzylic alcohols and amines besides enhancing the catalytic efficiency by ~1.5 fold. Additionally, the ability of this protocol to follow all laws of green chemistry, make this superior over other existing protocols. Detailed investigations of the reaction kinetics, surface chemistry, and quantum mechanics computations based on Density Functional Theory (DFT) were pursued to validate the feasibility of the reaction protocol.

Inspired by the surface defect mediated enhancement of oxidizability of meso-MnOx,[28] we selected a cationic dopant to maximize this property without changing its crystal structure. Therefore, the size of the metal dopant was supposed to be smaller or similar to that of Mn. Among all options Co was an obvious choice due to the i) ease of reducibility of Co^{3+} species (E°_{red} = + 1.81), and ii) excellent proton adsorption by both Co^{0} and Co^{2+} sites.[34] Interestingly, both Co^{2+} and Co^{3+} species are found to co-exist in mesoporous cobalt oxide which is known for its strong oxidizability.[35] Hence, we prepared cobalt (Co) doped meso-MnOx where Co was present as mesoporous cobalt oxide. To verify the presence of cobalt oxides on the surface of meso-MnOx, X-ray photoelectron spectroscopic (XPS) techniques were used, where an increasing peak intensity was observed with the increment of the percentage of the dopant (**Figure S4, b**). To estimate the impact of cobalt oxide modification on the meso-MnOx surface, further catalytic experiments were performed.

Table 1. Aerobic oxidative coupling of *benzylamine* and 4-methoxy benzylalcohol *to* selectively synthesize *unsymmetrical imines (I)* in the presence of different **catalysts**.[a]

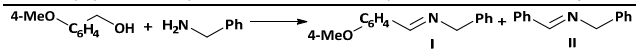

Entry	Catalyst	Conversion (%)[b]	Selectivity of I (%)[b]	TOF[c]
1.	No catalyst	10	20	N/A
2.	Meso-CoOx	41	96	0.64
3.	Meso-MnOx	68	71	1.06
4.	Meso-1%Co-MnOx	> 99	98	1.55
5.	Meso-3%Co-MnOx	88	97	1.38
6.	Meso-5%Co-MnOx	80	97	1.25
7.[d]	Meso-MnOx	93	78	1.45
8.[e]	Meso-MnOx	98	70	1.53

[a] Reaction conditions: benzylamine (0.5 mmol), 4-methoxy benzylalcohol (1.2 eqv.), Toluene (1 mL), 25 mg of catalyst (calcined up to 250 °C), 100 °C, 2 hours. [b] Conversions and selectivities were determined by GC-MS. [c] TOF = TON/ Time (h), TON = no of moles of limiting reagent converted to product per mole of catalyst. [d] 350 °C, [e] 450 °C.

A coupling reaction between benzylamine and benzylalcohol was considered as the model to verify the enhancement of activity upon cobalt doping. The cobalt oxide modified meso-MnOx surface exhibited better reactivity than bare meso-CoOx or meso-MnOx (**Table 1**, **entry 1-3**). To verify the role of Co in this process, its loading amount was optimized. The 1 mol % CoOx on meso-MnOx was the most active with > 99 % of conversion (**Table 1**, **entry 2-6**). Beyond this, a gradual decrease of imine formation was observed with increasing cobalt doping. This trend of conversion was found to be proportional to the content of surface active lattice oxygen, as revealed by the XPS analysis (**Table S1**). The surface area (**Figure S2**) of a material, which is a direct measure of active site density, also displayed a proportional relation with reaction conversions **(Table 1, S1** and **S2)**. These suggest that the surface active lattice oxygens, which proportionally varies with the surface area, are extremely critical to enhancing the reactivity of meso-Co-MnOx. However, this does not seem to be consistent with the poor catalytic activity of meso-CoOx, despite its high lattice oxygen content (**Table S1)**. This can be attributed to the higher metal-oxygen bond strength in CoOx as compared to MnOx. The impact of lattice oxygens was further noticed when reactivities of differently calcined meso-MnOx were compared. An increase in calcination temperature increased the lattice oxygen content (**Table 1**, **entry 9-10** and **Table S1**), which enhanced the conversion.

A continuous increase in product formation with increasing catalyst loading was obtained from the system (**Figure S7**), which indicated the absence of mass transfer limitations or adsorption. The screening of solvents and their volumes showed that one mL of toluene was the best combination to achieve conversion of 80 % (**Table S3** and **S4**). The increase in solvent volume probably lowered the collision frequency between the substrate and catalyst, which resulted in the declining yield (**Table S4**). The ratio of substrates was also optimized, where an excess of the alcohol over amine yielded the hetero-coupled product with better efficiency (**Table S5, entry 3**). This can be rationalized by the slower rate of alcohol oxidation than the homo-coupling of amine, as revealed by the obtained rate constants (**Table S8**). Moreover, the impact of reaction environment was understood as the reaction yield increased gradually with increasing the oxygen content of the atmosphere (**Table S6**). The yield increased from 66 % to > 99 % as the nitrogen atmosphere was replaced with oxygen. This was probably due to the facile replenishment of lattice oxygen vacancies by atmospheric oxygen. Hence, one mL of toluene as the solvent at 100 °C under oxygen environment was chosen to be optimal for the coupling reaction in the presence of the meso-1%Co-MnOx catalyst.

Scheme 1. Aerobic oxidative coupling of *amines* and *alcohols to* selectively synthesize *imines via cross-coupling (I).* [a]

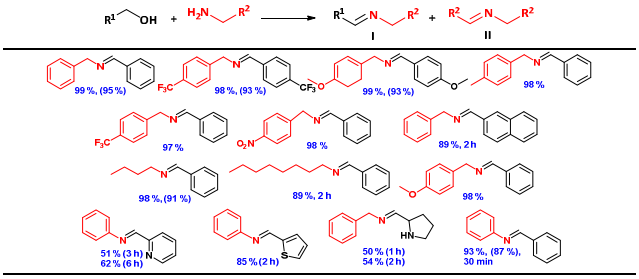

[a] Reaction conditions: amines (0.5 mmol), alcohols (1.2 eqv.), Toluene (1 mL), 25 mg of catalyst (1% Co-MnOx-250 °C), 2 h, 100 °C. Conversions and selectivities were determined by GC-MS. Selectivity of all cross-coupled imines were 98 %. Numbers depicted within parenthesis and without parenthesis are conversions and isolated yields.

These optimized reaction conditions were used to explore the substrate scope of this protocol. Almost all benzylamines and benzylalcohols were efficiently coupled (mostly above 98 %) to yield different asymmetric and symmetric imines (**Scheme 1**). Bulky reactants, such as 2-naphthylmethanol, suffered from a lower rate

View Article Online
DOI: 10.1039/C8GC00862K

of reaction than others (**Scheme 1**). Whereas, metal poisoning by heteroatoms caused inhibition of benzylamine to pyrrolidin-2-ylmethanol coupling yielding only 54 % (**Scheme 1**). However, no impact of i) the electronic nature of substituents, and ii) the aromaticity of reagents, was observed in the protocol (**Scheme 1**).

Scheme 2. Other aerobic oxidative processes.*

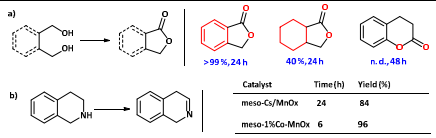

* Reaction conditions: a) Diol (0.5 mmol), n-Butanol (2 mL), 25 mg of 1% Co-MnOx-250 °C, 100 °C. b) 1,2,3,4-tetrahydroisoquinoline (0.5 mmol), toluene (0.5 mL), 25 mg of 1% Co-MnOx-250 °C, 100 °C. Selectivity of all cross-coupled imines were > 99 %. Conversions and selectivities were determined by GC-MS.

The enhanced oxidizability of the meso-Co-MnOx catalyst was further validated as the relatively difficult oxidation of benzene-1,2-dimethanol to lactone, which is not possible by bare meso-MnOx, was achieved feasibly (**Scheme 2. a, Table S10**). This oxidation process is highly dependent on the distance between its aliphatic branches, which causes difficulty in expanding the substrate scope (**Scheme 2. a**). The transformation of relatively inert secondary amine (1,2,3,4-tetrahydroisoquinoline) to the corresponding imine, also evidenced a ~4 times higher catalytic activity for meso-1%Co-MnOx than the previously reported meso-MnOx catalyst (**Scheme 2. b**).[29] Thereby, both of these systems support the enhanced oxidizability of meso-1%Co-MnOx catalyst.

Scheme 3. Reductive transformation of *imines* to *amines*. [a]

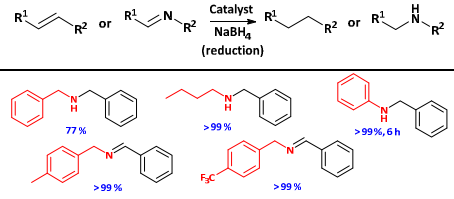

[a] Reaction conditions: imine (0.5 mmol), Toluene (2 mL), 25 mg of catalyst (5% Co-MnOx-250 °C), $NaBH_4$ (1 eqv.), 5h, and 100 °C. Selectivity of all cross-coupled imines were > 99 %. Conversions and selectivities were determined by GC-MS.

Scheme 4. Reductive coupling of imines to *amines* and *alcohols* in the presence of 10% Co-MnOx. [a]

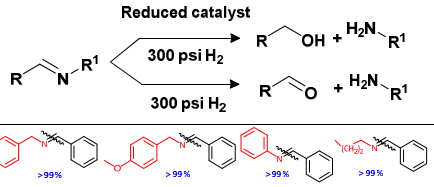

[a] Reaction conditions: imine (0.5 mmol), Toluene (2 mL), 25 mg of catalyst (1% Co-MnOx-250 °C), 300 psi, 6 h, 100 °C. Selectivity of all cross-coupled imines were > 99 %. Conversions and selectivities were determined by GC-MS.

To explore the reducibility of the system, transformation of benzylidene phenyl imine to the corresponding secondary amine was selected as a model reaction. By optimizing the reaction conditions, meso-5%Co-MnOx was found to be the best catalyst in the presence of a reducing agent $NaBH_4$ (**Table S7**, **entry 1**). Moreover, using these optimized conditions, various amines were converted to their corresponding imines with excellent yield (mostly > 99 %) (**Scheme 3**). However, under high pressure of hydrogen (300 PSI), all imines were completely (> 99 %) degraded to their corresponding amines and alcohols (**Scheme 4**). This superior oxidizability and efficient reducibility of the catalyst depicts its dual catalytic behavior (**Scheme 1-4**).

Most heterogeneous systems suffer from i) the leaching of active metals in solution, and ii) the deactivation of the active sites due to adsorption or aggregation of nanoparticles. To study the leaching of active metals, a hot filtration test (**Figure S7**) and the reusability of the catalyst (**Figure S8**) were evaluated. In the hot filtration test, the catalyst was separated from the system after 30 minutes (at about 37 % conversion), and the filtrate was reinstated under the same reaction conditions for another 30 minutes. No significant improvement in imine formation after catalyst separation confirmed the absence of active metal species in the solution. Whereas, to determine reusability, the retrieved catalyst was washed and reactivated at 250 °C for 1 hour, before reuse, to remove adsorbed foreign molecules. These post-reaction treatments were repeated with the catalyst after every cycle for the next five cycles until the conversion decreased by ~20 % of its initial activity (**Figure S8, a**). An X-ray diffraction study on the catalyst after the 5th cycle was performed to confirm the preservation of its amorphous nature (**Figure S8, b**). This categorized our catalytic system to be genuinely heterogeneous, stable, and reusable.

The excellent catalytic activity of the system, motivated us to investigate the reaction kinetics and surface chemistry. A time-dependent study was performed by continuous sampling from the reaction mixture at 100 °C over a period. This revealed a first-order rate equation, with a rate constant (k) of 0.02 min^{-1}, as compared to the benzylamine (**Figure S11**). To evaluate the apparent activation energy of 31 KJ/mol from Arrhenius plot, several time-dependent reactions were performed in a temperature range of 30-120 °C (**Figure S12**).

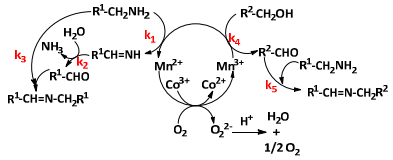

k_1, k_2, k_3, k_4, and k_5 are the rate constant of specified steps

Scheme 5. The overall reaction mechanism for the coupling of amine and alcohols to imines.

The above-mentioned experimental findings led us to propose a mechanism to explain the present catalytic protocol. Control experiments and characterization such as H_2-TPR (temperature programmed reduction) and XPS were used to understand the surface chemistry. Learning from our previous findings,[30,31] a radical pathway involving an electron transfer from the adsorbed amine to the metal center is believed to initiate the reaction. Sequential elimination of C–H and N–H protons is reported to cause the formation of RCH=NH, which after hydrolysis forms RCH=O.[29] These aldehydes upon coupling with amines produced symmetric imines **(Scheme 5)**. Whereas, the aldehydes generated from the alcohols are coupled to amines to yield asymmetric imines **(Scheme 5)**. However, the challenges to understanding i) the enhanced activity

View Article Online
DOI: 10.1039/C8GC00862K

of meso-Co-MnOx over meso-MnOx, and ii) the dominance of hetero-coupling during the reaction. Therefore, the two-step reaction mechanism, consisting of dehydrogenation and dehydration, for imine formation requires more investigation.

As discussed before, the correlation between the conversion and lattice oxygen content indicated the importance of lattice oxygens during the reaction (**Table 1 and S1**). The excellent reactivity of manganese (Mn^{3+}) oxides can be attributed to the elongation of Mn-O bonds due to a Jahn–Teller (*J–T*) distortion,[36] which assists the formation of OH radicals. The presence of additional Co^{2+} ions in meso-MnOx, also facilitates this metal-O bond elongation, contributing to the OH radical content. Therefore, the presence of Co^{2+} in meso-MnOx not only increases the lattice oxygen content due to enhanced surface defects but also the content of reactive oxygen species.

To understand the dominance of hetero-coupling over homo-coupling, several control experiments were performed. This revealed faster kinetics (by ~50 times) of homo-coupling of amines by meso-MnOx (k= 0.02 min^{-1}) than with meso-CoOx (k= 0.0004 min^{-1}) (**Table S8**). This slow reactivity in the presence of CoOx impacted the result of Co doped meso-MnOx systems by decreasing the reactivity about ~9-18 times than that of meso-MnOx (k= 0.0011–0.0023 min^{-1}) (**Table S8**). This suppressed rate of homo-coupling resulted in a better selectivity of hetero-coupling. Interestingly, the observed rate (k= 0.0198 min^{-1}) of benzylalcohol - benzylamine coupling reaction was found to be ~3 times slower than the benzaldehyde - benzylamine coupling reaction (**Table S8, Figure S10**). This indicates the presence of a different mechanistic pathway which involves intermediates other than imines (RCH=NH) and aldehydes (RCH=O) as proposed before.

A detailed investigation was carried out to identify the reactive oxygen species (ROS) formed during the reaction. According to the possible ROS pathway,[37] molecular oxygen is converted to water through the sequential formation of superoxide anion, hydrogen peroxide, and hydroxyl radical. Therefore, specific additives were used to generate characteristic fluorescence or UV-vis peak from different ROS, to identify them. The superoxide anion was detected by the characteristic UV-Vis peak in between 450-700 nm in the presence of nitro tetrazolium blue chloride (NBT) additive (**Figure S5. a**).[38] Whereas, an increasingly intense characteristic UV-Vis peak (at 596 nm, in the presence of leuco crystal violet) confirmed the presence of hydrogen peroxide (**Figure S5. b**) during the reaction.[39] The hydroxyl radical was detected by the characteristic fluorescent peak at 430 nm in the presence of disodium terephthalate (DST) (**Figure S5. c**).[40] The identification of two ROS in a single reaction, required the detection of the terminal ROS. Consequently, ROS quenchers curcumin,[41] and butylated hydroxytoluene (BHT)[42] were introduced to terminate both superoxide anion and hydroxyl radical, respectively. The quenching of hydroxyl radicals inhibited the formation of imines (**Figure S5. D, entry 2**). Whereas, a considerable amount (~15 %) of imine was obtained, despite quenching superoxide anions (**Figure S5. d, entry 1**). This confirmed the hydroxyl radical to be the terminal ROS.

To understand this reaction mechanism and validate the role of Co in meso-MnOx, computational calculations using density functional theory (**DFT**) were performed as implemented in the Vienna *ab initio* Simulation Package (**VASP**).[43,44] The generalized gradient approximations (such as Perdew, Burke, and Ernzerhof (PBE) functionals),[45] and Hubbard U correction [46] on the d-orbitals of Mn and Co were used to estimate the total energies of all configurations, from reactants to intermediates to products. Our primary intention was to determine the reaction mechanism and identify the source of the faster kinetics of meso-MnOx in the presence of Co doping (**Table 1, Table S8**).

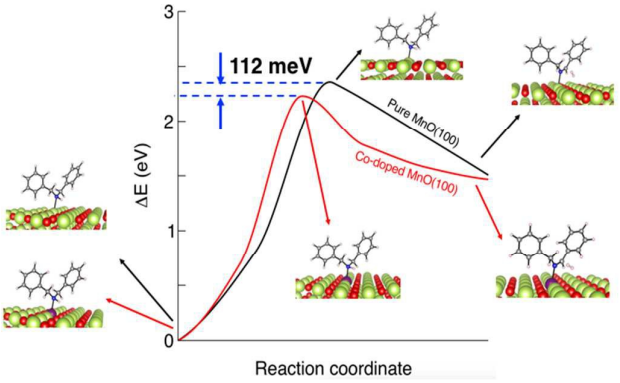

Figure 1. The black and red curves represent the energy profiles of benzylamine to benzyl alcohol coupling reaction on (100) plane of meso-MnOx and meso-Co-MnOx in the gas phase, respectively. In this DFT computed comparison, optimized geometries of the reactant, transition state, and product were used for both cases. ΔE: The energy difference of the reactant, transition state, and product to the corresponding reactants for MnO and Co-doped MnO surface. Green, purple, red, grey, blue and while balls denote the Mn, Co, O, C, N and H atoms, respectively.

According to these calculations, the reaction occurred in two main steps. In the first step, a condensation reaction between $PhCH_2NH_2$ and $PhCH_2OH$ led to the formation of corresponding secondary amine, which lost a molecule of H_2 in the rate determining step (the second step) to produce the desired imine. Therefore models were prepared to capture energetics of all intermediates of this step. A comparison between the DFT energy profiles of meso-MnOx and meso-1%Co-MnOx in the gas phase show a lowering of the activation barrier upon introducing Co in meso-MnOx (by 112 meV or 2.58 kcal/mol) (**Figure 1**). This lowering of the activation barrier was assumed to be responsible for enhancing the reaction by ~1.5 times. Also, all intermediates were found to bind with the MnO surface through the nitrogen of benzylamines. These findings led us to propose a mechanism which supports the existence of hydroxyl radicals, the formation of aldehydes (during the homo-coupling of amines), and the presence of a negatively charged intermediate (**Figure S13**). [29]

We propose the formation of RCH=NH (for homo coupling) and RCH_2N=CHR (for hetero-coupling) can be done either by abstracting H from corresponding amine using OH radical (***path a***) or by a sequential elimination of e^- and H^+ (***path b***). Ideally, ***path b*** should be more time-consuming than ***path a*** due to the involvement of multiple steps. This suggests the involvement of ***path b*** in benzylamine -benzylalcohol coupling, as the observed rate (k= 0.0198 min^{-1}) was found to be significantly lower than the anticipated rate (from benzaldehyde - benzylamine coupling) (**Table S8)**.

In summary, we have successfully developed a cobalt doped mesoporous manganese oxide material with enhanced oxidizability

View Article Online
DOI: 10.1039/C8GC00862K

and selectivity. This mesoporous material with a surface area of 81 m^2/g and monomodal pore-size distribution (pore diameter 3.4 nm) was found to have a high content of lattice oxygen and multi-valency of both Co and Mn. The meso-1%Co-MnOx system exhibited an enhanced activity (by ~1.5 times) as compared to the un-doped meso-MnOx material. This was also observed during the relatively robust oxidation of diols and 1,2,3,4-tetrahydroisoquinoline to their corresponding lactones and imine, respectively (**Scheme 2**). The enhanced efficiency of this catalyst was supported by the lowest reduction temperature as revealed from H_2-TPR (**Figure S14**). Most importantly, the unprecedented result of cross-coupling reaction with > 99 % selectivity was truly surprising. In contrast to this excellent activity, i) facile reduction of imines to amines in the presence of $NaBH_4$; and ii) transformation of imines to its parent alcohols and amines, revealed the applicability of this catalyst. Therefore in the absence of ligands, additives, bases, and precious metals; this economical and sustainable heterogeneous system is superior to the existing ones. The combined effect of multivalent metal species and lattice oxygen was found to be critical for the enhanced reactivity and excellent selectivity. DFT computations were utilized to estimate the relative total energies of the rate determining step and propose a reaction mechanism which supports experimental findings. We intend to continue our investigations to understand further details of the surface chemistry and identify the role of other surface defects, such as oxygen-vacancy.

Conflicts of interest

There are no conflicts of interest to declare

Acknowledgements

S.L.S. is grateful for support of the U.S. Department of Energy, Office of Basic Energy Sciences, Division of Chemical, Biological and Geological Sciences under Grant DE-FG02-86ER13622.A000. The TEM studies were performed using the facilities at the UCONN/FEI Center for Advanced Microscopy and Materials Analysis (CAMMA).

Keywords

Mesoporous materials · Manganese oxide · Cobalt oxide · Alcohol - Amine coupling · Heterogeneous catalysis · Aerobic oxidation.

Notes and References

1 R. W. Layer, *Chem. Rev.*, 1966, **63**, 489–510.
2 S. Kobayashi, Y. Mori, J. S. Fossey and M. M. Salter, *Chem. Rev.*, 2011, **111**, 2626–2704.
3 M. E. Belowich and J. F. Stoddart, *Chem. Soc. Rev.*, 2012, **41**, 2003–2024.
4 S. Kobayashi and H. Ishitani, *Chem. Rev.*, 1999, **99**, 1069–1094.
5 H. Naeimi, F. Salimi and K. Rabiei, *J. Mol. Catal. A Chem.*, 2006, **260**, 100–104.
6 B. Chen, L. Wang and S. Gao, *ACS Catal.*, 2015, **5**, 5851–5876.
7 C. M. Wong, R. T. McBurney, S. C. Binding, M. B. Peterson, V. R. Gonçales, J. J. Gooding and B. A. Messerle, *Green Chem.*, 2017, **19**, 3142–3151.
8 K. C. Nicolaou, C. J. N. Mathison and T. Montagnon, *Angew. Chemie Int. Ed.*, 2003, **42**, 4077–4082.
9 T.-L. Ho, *Tandem organic reactions*, Wiley, 2015.
10 M. Largeron and M.-B. Fleury, *Angew. Chem. Int. Ed.*, 2012, **51**, 1–5.
11 M. Largeron and M.-B. Fleury, *Science* 2013, **339**, 43–4.
12 B. Chen, J. Li, W. Dai, L. Wang and S. Gao, *Green Chem.*, 2014, 3328–3334.
13 H. Sun, F.-Z. Su, J. Ni, Y. Cao, H.-Y. He and K.-N. Fan, *Angew. Chem. Int. Ed.*, 2009, **48**, 4390–4393.
14 J. Mielby, R. Poreddy, C. Engelbrekt and S. Kegnæs, *Chinese J. Catal.*, 2014, **35**, 670–676.
15 L. Jiang, L. Jin, H. Tian, X. Yuan, X. Yu and Q. Xu, *Chem. Commun.*, 2011, **47**, 10833–10835.
16 W. He, L. Wang, C. Sun, K. Wu, S. He, J. Chen, P. Wu and Z. Yu, *Chem. - A Eur. J.*, 2011, **17**, 13308–13317.
17 J. W. Kim, J. He, K. Yamaguchi and N. Mizuno, *Chem. Lett.*, 2009, **38**, 920–921.
18 S. Sithambaram, R. Kumar, Y.-C. Son and S. L. Suib, *J. Catal.*, 2008, **253**, 269–277.
19 G. Jaiswal, V. G. Landge, D. Jagadeesan and E. Balaraman, *Green Chem.*, 2016, **18**, 3232–3238.
20 B. L. Ryland and S. S. Stahl, *Angew. Chem. Int. Ed.*, 2014, **53**, 8824–8838.
21 M. Tamura and K. Tomishige, *Angew. Chem. Int. Ed.*, 2015, **54**, 864–867.
22 H. Wang, J. Zhang, Y.-M. Cui, K.-F. Yang, Z.-J. Zheng and L.-W. Xu, *RSC Adv.*, 2014, **4**, 34681–34686.
23 S. Samanta, S. Khilari, D. Pradhan and R. Srivastava, *ACS Sustain. Chem. Eng.* , 2017, **5**, 2562−2577.
24 M. A. Berliner, S. P. A. Dubant, T. Makowski, K. Ng, B. Sitter, C. Wager and Y. Zhang, *Org. Process Res. Dev.*, 2011, **15**, 1052–1062.
25 H. Huang, J. Huang, Y.-M. Liu, H.-Y. He, Y. Cao and K.-N. Fan, *Green Chem.*, 2012, **14**, 930–934.
26 P. Anastas and N. Eghbali, *Chem. Soc. Rev.*, 2010, **39**, 301–312.
27 A. E. Wendlandt and S. S. Stahl, *J. Am. Chem. Soc.*, 2014, **136**, 506–512.
28 S. Biswas, B. Dutta, A. Mannodi-Kanakkithodi, R. Clarke, W. Song, R. Ramprasad and S. L. Suib, *Chem. Commun.*, 2017, **53**, 11751–11754.
29 S. Biswas, B. Dutta, K. Mullick, C.-H. Kuo, A. S. Poyraz and S. L. Suib, *ACS Catal.*, 2015, **5**, 4394–4403.
30 B. Dutta, S. Biswas, V. Sharma, N. O. Savage, S. P. Alpay and S. L. Suib, *Angew. Chem.*, 2016, **55**, 2171–2175.
31 B. Dutta, V. Sharma, N. Sassu, Y. Dang, C. Weerakkody, J. Macharai, R. Miao, A. Howell and S. L. Suib, *Green Chem.*, 2017, **19**, 5350–5355.
32 X. Li, T. Lunkenbein, V. Pfeifer, M. Jastak, P. K. Nielsen, F. Girgsdies, A. Knop-Gericke, F. Rosowski, R. Schlogl and A. Trunschke, *Angew. Chem. Int. Ed.*, 2016, **55**, 4092–4096.
33 S. L. Suib, *J. Mater. Chem.*, 2008, **18**, 1623–1631.
34 P. Van Helden, J.-A. Van Den Berg and C. J. Weststrate, *ACS Catal.* , 2012, **2**, 1097−1107.

View Article Online
DOI: 10.1039/C8GC00862K

35 N. Bingwa, S. Bewana, M. J. Ndolomingo, N. Mawila, B. Mogudi, P. Ncube, E. Carleschi, B. P. Doyle, M. Haumann and R. Meijboom, *Appl. Catal. A Gen.*, 2018, **555**, 189–195.
36 U. Maitra, B. S. Naidu, A. Govindaraj and C. N. R. Rao, *Proc. Natl. Acad. Sci.*, 2013, **110**, 11704–11707.
37 R. Rodriguez and R. Redman, *Proc. Natl. Acad. Sci.*, 2005, **102**, 3175–3176.
38 C. J. F. Van Noorden and R. G. Butcher-F, *Anal. Biochem.*, 1989, **176**, 170–174.
39 C. A. Cohn, A. Pak, D. Strongin and M. A. Schoonen, *Geochem. Trans.*, 2005, **6**, 47–51.
40 A. Gomes, E. Fernandes and J. L. F. C. Lima, *J. Biochem. Biophys. Methods*, 2005, **65**, 45–80.
41 T. Ak and I. Gülçin, *Chem. Biol. Interact.*, 2008, **174**, 27–37.
42 J. Wang, Y. Guo, B. Liu, X. Jin, L. Liu, R. Xu, Y. Kong and B. Wang, *Ultrason. Sonochem.*, 2011, **18**, 177–183.
43 G. Kresse and J. Furthmü, *Phys. Rev. B*, 1996, **54**, 11169–11186.
44 G. Kresse Av and J. Furthmiiller, *Comput. Mater. Sci.*, 1996, **6**, 15–50.
45 J. P. Perdew, K. Burke and M. Ernzerhof, *Phys. Rev. Lett.*, 1996, **77**, 3865–3868.
46 S. L. Dudarev, G. A. Botton, S. Y. Savrasov, C. J. Humphreys and A. P. Sutton, *Phys. Rev. B*, 1998, **57**, 1505–1509.

View Article Online
DOI: 10.1039/C8GC00862K

Graphical Abstract:

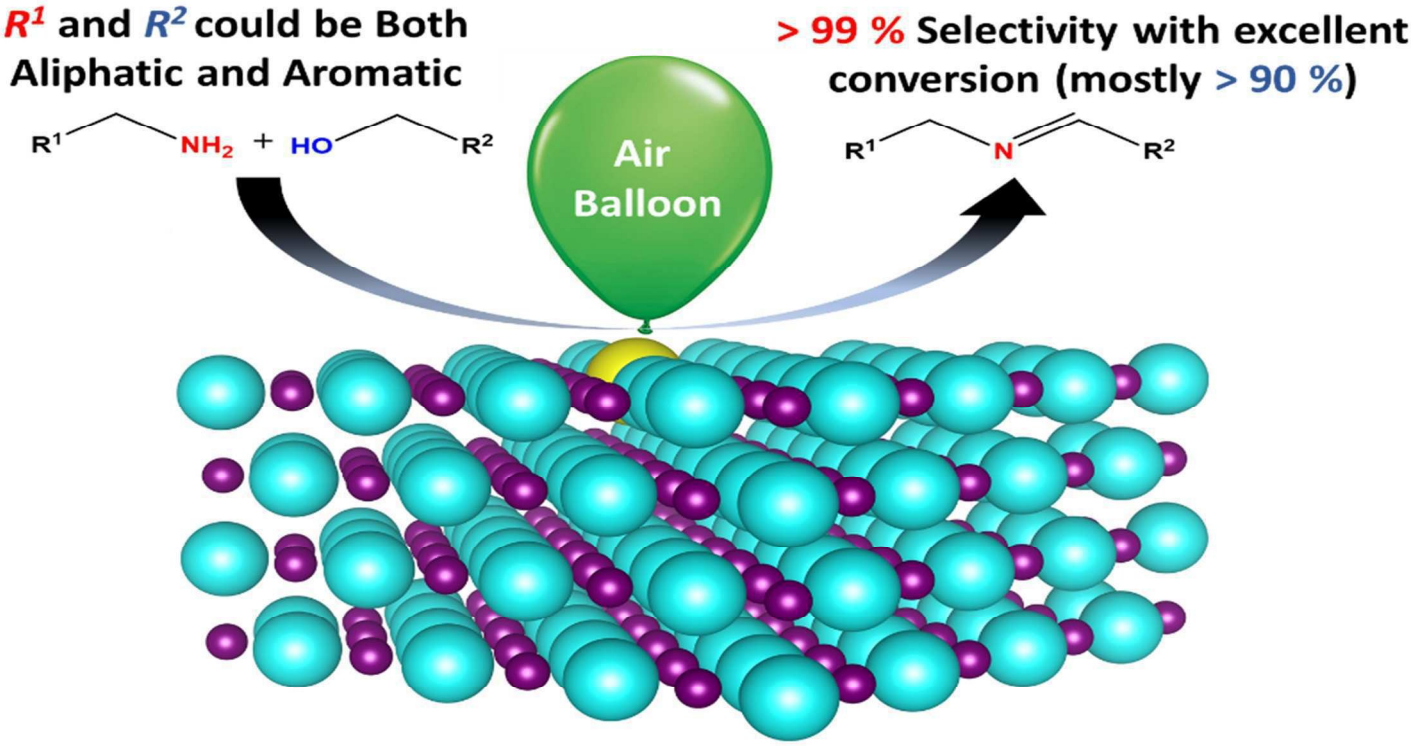

Cobalt doped mesoporous manganese oxide: An excellent oxidative catalyst (for producing asymmetric imines with >98% selectivity) with significant reductive properties.